Nanomorphology of Polymer Frameworks and their Role as Templates for Generating Size-Controlled Metal Nanoclusters

Frederica Artuso,[a] Angelo A. D'Archivio,[b] Silvano Lora,[c] Karel Jerabek,[d] Milan Králik,[e] and Benedetto Corain*[a]

Abstract: The microporous (gel-type) functional resin co-poly-*N*,*N*-dimethylacrylamide (DMAA) (88% mol)/methacrylic acid (MAA) (8% mol)/*N*,*N*′-methylenebisacrylamide (MBAA) (4% mol) (MPIF(H)) is employed as the hosting framework for the production of resin-supported Pd^0 nanoclusters. The obtained composite $MPIF^-Na^+/Pd^0$ is prepared upon reducing, in ethanol, $MPIF^-Pd^{2+}{}_{0.5}$, obtained upon previous homogeneous dispersion of "Pd^{2+}" inside the resin particles (XRMA control) through ion-exchange. Metal nanoclusters appear to be size-controlled (2.0 ± 0.2 nm) and are seen to reasonably fit the predominant resin "nanopores" diameter, determined in ethanol (3.2 nm) by means of inverse steric exclusion chromatography (ISEC).

Keywords: nanoclusters · nanostructures · gel-type resins · palladium

Introduction

We have been active during the last decade in elucidating the molecular bases of some industrial catalysts based on palladium(0) supported on functional resins that were discovered and commercialized by Bayer AG in the sixties and early seventies.[1–3] When we entered the field,[4] we were struck by the incredible paucity of relevant published data available in the literature and by the great potentialities embodied in this family of catalysts, in which the chemical potency of active metals nanoclusters may be conjugated with the fine physico-chemical features of the macromolecular support.[5–7]

We note that our work has contributed to the rationalization of metallation and reduction protocols,[3] as well as to the quantitative evaluation of nanomorphology and molecular accessibility of the polymer frameworks.[6]

We have recently published in this journal both on results relevant to the exploitation of fine physico-chemical features of the polymer framework to act on the selectivty of the catalyst as a whole[8], and on results relevant to the technological value of these catalysts in terms of resistance to hydrogenolysis and to mechanical attrition.[9] We wish to report now on another fine feature of these catalysts, that is, the size of the metal clusters contained inside them when the catalyst is activated upon reduction of Pd^{II} to Pd^0.

Just few years ago we noticed that 4% mol cross-linked gel-type resins seemed to be able to control in some way the the size of Pd^0 nanoclusters generated inside of their polymer framework,[10] and we started in 1997 a project aimed at providing an insight into this attractive aspect of resins chemistry and physics. The working hypothesis stemming from the preliminary results reported in reference [11] is illustrated in Figure 1.

The polymer framework of a gel-type resin produced in the presence of a 2–8% mol bifunctional co-monomer (the cross-linker) can be depicted as a three-dimensional mesh system made of intercommunicating "cavities", a two-dimensional section of which is depicted in Figure 1. The picture illustrates a section of a spheroidal volume element with a diameter equal to about 15 nm in which the polymer chains are drawn in scale with their effective diameter of 0.4 nm. Cavities in this

[a] Prof. B. Corain, F. Artuso
Istituto di Scienze e Tecnologie Molecolari
C.N.R., Sezione di Padova
c/o Dipartimento di Chimica Inorganica Metallorganica Analitica
Via Marzolo 1, 35131 Padova (Italy)
Fax: (+49) 827-5223
E-mail: benedetto.corain@unipd.it

[b] Dr. A. A. D'Archivio
Dipartimento di Chimica Ingegneria Chimica e Materiali
Università di L'Aquila, Via Vetoio Coppito Due
67010 L'Aquila (Italy)

[c] Dr. S. Lora
Istituto per la Sintesi Organica e la Fotoreattività, C.N.R., via Romea 4
35020 Legnaro (Italy)

[d] Dr. K. Jerabek
Institute of Chemical Process Fundamentals
Rozvojova 135, 16502 Suchdol, Praha 6 (Czech Republic)

[e] Dr. M. Králik
Department of Organic Technology
Slovak University of Technology
Radlinskeho 9, 812 37 Bratislava 1 (Slovak Republic)
E-mail: kralik@chtf.stuba.sk

DOI: 10.1002/chem.200304965

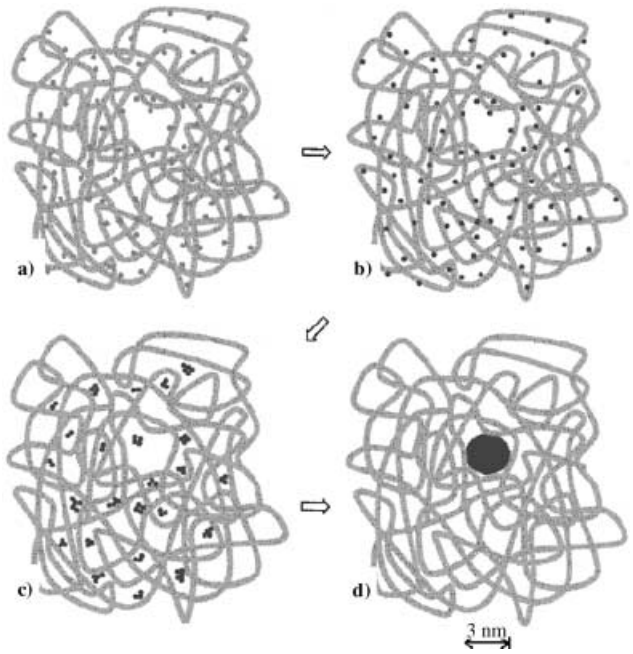

Figure 1. Model for the generation of size-controlled metal nanoparticles inside metallated resins. a) Pd^{II} is homogeneously dispersed inside the polymer framework; b) Pd^{II} is reduced to Pd^0; c) Pd^0 atoms start to aggregate in subnanoclusters; d) a single 3 nm nanocluster is formed and "blocked" inside the largest mesh present in that "slice" of polymer framework.

framework have a lumen ranging from 0.6 to 3.0 nm. This qualitative and quantitative picture is provided by porosimetric analysis by means of inverse steric exclusion chromatography (ISEC).[12] A geometrically simple quantitative description of pore morphology of a given swollen polymer framework is provided by the so-called Ogston's model,[13] which depicts pores as spaces among randomly oriented cylindrical rods. A pictorially useful geometric representation of the system of cavities defining the polymer framework is also provided by the conventional cylindrical pores model.[14] In this context, it is important to stress that depicting pores in the swollen gel as cylindrical holes featuring a solid matter may produce incorrect information as far as the specific pore volume is concerned. Moreover, owing to the intrinsic irregularity of the size of the spaces located among expanded polymer chains,[5] the framework will turn out to be described as if it were built up with cavities of different size, but some of them may be more abundant than others (this is in fact the case of our material $MPIF^-Na^+/Pd^0$, see Table 1) and, therefore, conditioning the predominant size of the obtained metal nanoclusters.

The working hypothesis expressed by Figure 1 can now be illustrated in the following terms. Pd^0 atoms are generated isotropically in every domain of the polymer framework and they tend to freely aggregate to growing metal nanoclusters that can move through the spheroidal volume until the nanocluster reaches the largest mesh available in that volume. At this point the size control inside of the spheroidal space volume is achieved. Off course the same can be said for all other volume elements of the polymer framework, and, at the very end, the size of the observed metal nanoclusters will be dictated by the size of the largest and most abundant three-dimensions meshes ("cylindrical pores") available in the whole of the body of a given resin particle.

Table 1. Rotational mobility data of TEMPONE moving inside our investigated materials, after swelling in water and ethanol.

Solvent	Sample	τ 25 °C [ps ± 5 %] [a]	a_N [G ± 0.03 G] [b]	E_a [kJ mol^{-1} ± 0.5] [c]
	bulk	13	15.85	18.0
	MPIF(H)	91	15.73	23.5
water	$MPIF^-Na^+$	51	15.89	24.1
	$MPIF^-Pd^{2+}{}_{0.5}$	93	15.71	24.2
	$MPIF^-Na^+/Pd^0$	75	15.73	23.9
	bulk	21	14.88	13.4
	MPIF(H)	87	14.83	22.7
ethanol	$MPIF^-Na^+$	77	14.83	22.1
	$MPIF^-Pd^{2+}{}_{0.5}$	85	14.83	23.4
	$MPIF^-Na^+/Pd^0$	79	14.83	22.8

[a] Rotational correlation time. [b] ^{14}N isotropic hyperfine coupling constant. [c] Arrhenius activation energy of rotational diffusion.

This paper aims at a critical confirmation of results and arguments presented above and roughly anticipated in reference [11]. To this end a slightly different polymer backbone was utilized and a careful nano-morphological (ISEC and ESR) control was carried out in the materials involved in the two synthetic steps [Eq. (1) and (2)] :

$$\text{resin(H)} + 0.5\,Pd(OAc)_2 \overset{-AcOH}{\rightarrow} \text{resin}^-Pd^{2+}{}_{0.5} \quad (1)$$

$$\text{resin}^-Pd^{2+}{}_{0.5} \overset{+NaBH_4}{\rightarrow} \text{resin}^-Na^+/Pd^0{}_{0.5} + \text{products} \quad (2)$$

Results and Discussion

The co-polymerization of *N*,*N*-dimethylacrylamide (DMAA) (ca. 88 % mol), methacrylic acid (MAA) (ca. 8 % mol) and *N*,*N*′-methylenebisacrylamide (MBAA) (ca. 4 % mol) under γ-ray irradiation[7] at room temperature affords a gel-type resin, after suitable working up, as transparent, robust microparticles that are used after sieving (180–400 μm). The polymerization yield is greater than 96 %. The resin will be named hereafter as MPIF(H). SEM analysis exhibits the expected compact structure down to the maximum magnification available to the instrument. The resin undergoes facile palladiation with $Pd(OAc)_2$ ($MPIF^-Pd^{2+}{}_{0.5}$, brown) and subsequent reduction with excess $NaBH_4$ in absolute ethanol to give $MPIF^-Na^+/Pd^0$, (dark black), according to consolidated procedures[7, 11]. Both $MPIF^-Pd^{2+}{}_{0.5}$ and $MPIF^-Na^+/Pd^0$ were analyzed with XRMA (Figure 2).

Notice the remarkable homogeneity of Pd distribution (resolution power is ca. 5 μm) before and after metal reduction). XPS analysis fits the presence of only Pd^0 metal centers with no evidence of Pd^{II} species ($E_{Pd3d5/2} = 335.4$ eV and $E_{Pd3d3/2} = 340.8$ eV)[15]. E_{N1s}, E_{O1s}, and E_{C1s} do not change appreciably from MPIF(H) to $MPIF^-Pd^{2+}{}_{0.5}$ to $MPIF^-Na^+/Pd^0$.

Low-resolution TEM pictures of $MPIF^-Na^+/Pd^0$ microparticles (two different inspected fields) (Figure 3) reveal that

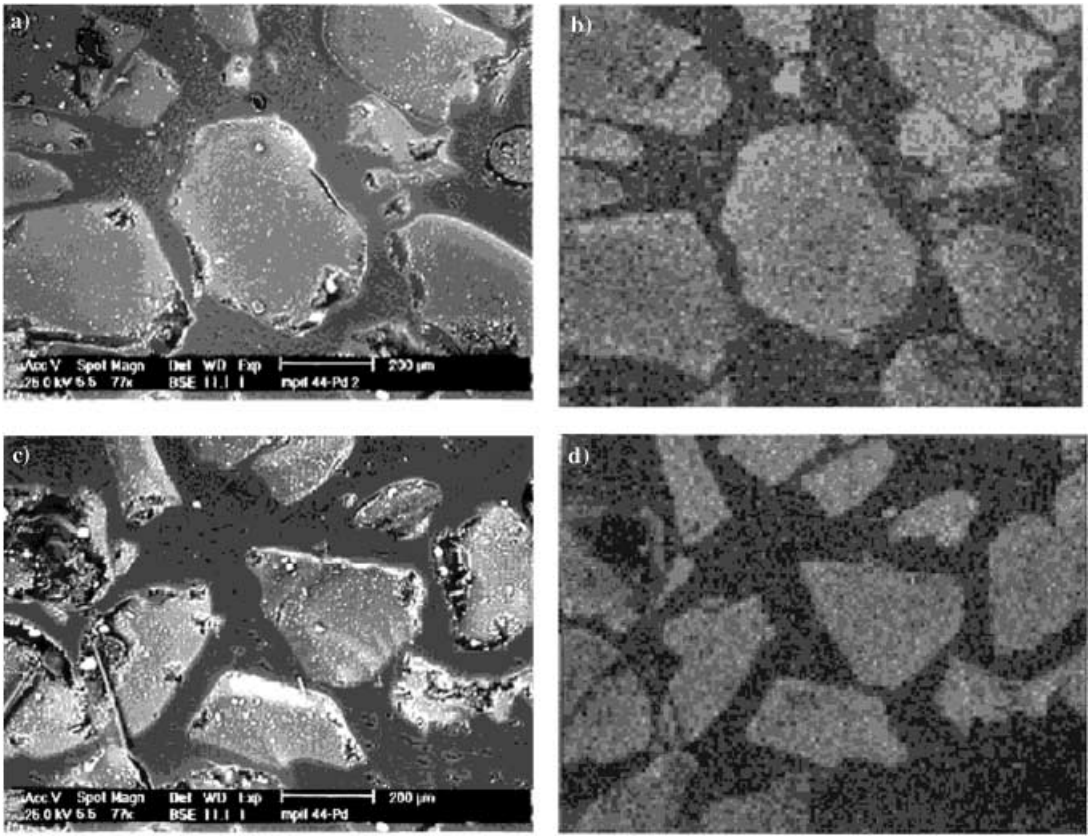

Figure 2. Palladium distribution through a section of $MPIF^{-}Pd^{2+}_{0.5}$ and $MPIF^{-}Na^{+}/Pd^{0}$ particles. Top: SEM picture (left) and XRMA scanning picture (right) of $MPIF^{-}Pd^{2+}_{0.5}$. Bottom: SEM picture (left) and XRMA scanning picture (right) of $MPIF^{-}Na^{+}/Pd^{0}$.

Pd nanoclusters are evenly distributed inside the inspected area and their size distribution is centred around 2 nm in diameter. HRTEM analysis reveals that the inter-row distance in Pd nanoclusters is close to 0.2 nm, in good agreement with literature data.[16]

The correlation of these dimensional observations with the nanomorphology of resins MPIF(H), $MPIF^{-}Pd^{2+}_{0.5}$, $MPIF^{-}Na^{+}$, and $MPIF^{-}Na^{+}/Pd^{0}$ requires detailed information on their swollen-state morphology. The best swelling medium for this would be of course ethanol, in which the generation of the Pd nanoclusters actually occurs. Unfortunately, it is impossible to perform ISEC measurements in ethanol, owing to a serious risk of enthalpic interaction of the standard solutes (steric probes) with the polymer matrix.[12, 14] Consequently, we carried out an ISEC investigation in an aqueous environment.

In order to evaluate the relevance of the analysis in water to the resins nanostructure in ethanol, ISEC analysis was preceded by an ESR investigation in ethanol and in water.[17, 18] In fact, we have shown that the rotational mobility of the spin probe TEMPONE (2,2,6,6-tetramethyl-4-oxo-1-oxyl-piperidine) in these and other solvents can be reliably correlated just with resins nanostructure stemming from ISEC in the same solvents. The relevant rotational mobility data are collected in Table 1.

Table 1 reveals that the relevant crucial parameters in both solvents, that is, correlation times of rotational diffusion τ, are very close to each other in water and ethanol, especially for $MPIF^{-}Na^{+}/Pd^{0}$. The temperature dependence of τ, as expressed by an apparent Arrhenius activation energy E_a, which in bulk media reflects the different temperature dependence of viscosity of water and ethanol, also converges when water and ethanol are confined inside the different materials. On the other hand, polarity experienced by the spin probe inside the polymer network is comparable with that of pure solvent, as demonstrated by the practical constancy of the ^{14}N isotropic hyperfine coupling constant a_N of both media.

It can be concluded that, while diffusion substantially occurs in the liquid medium confined inside of the polymer network, the same polymer framework moderately influences the mechanism of TEMPONE reorientation. This effect, as witnessed by the increase in E_a, is comparable in water and ethanol and can be ascribed to polymer chain motions that hinder the spin-probe diffusion more and more as temperature increases.

Consequently, this finding supports the reasonable assumption that the nanomorphologies of the polymer framework of $MPIF^{-}Na^{+}/Pd^{0}$ in water and alcohol are practically identical. This important statement makes the ISEC data reported in Table 2 particularly relevant.

It is seen that $MPIF^{-}Na^{+}$, the ultimate template able to control the nanoclusters size (see Introduction), is characterized by 3.2 nm cylindrical pores; compared with diameters of 1.8–2.4 nm observed for Pd nanoclusters. Consequently, the close similarity of the predominant pore diameter observed in water (ca. 3 nm) and the predominant metal-nanocluster

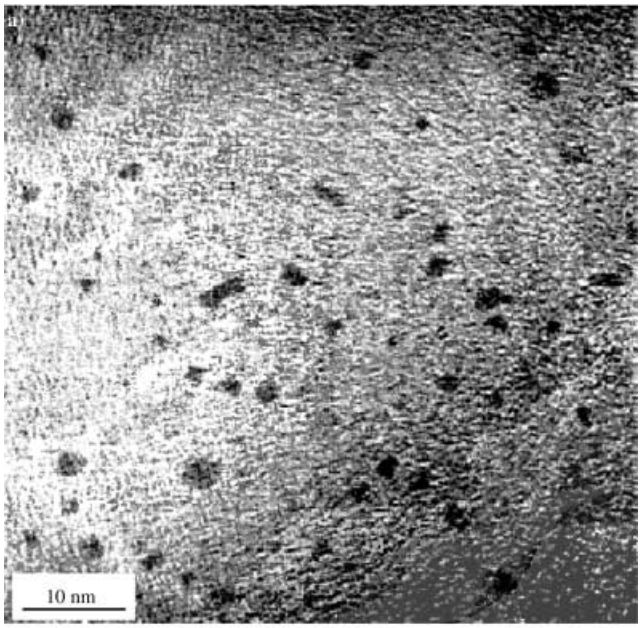

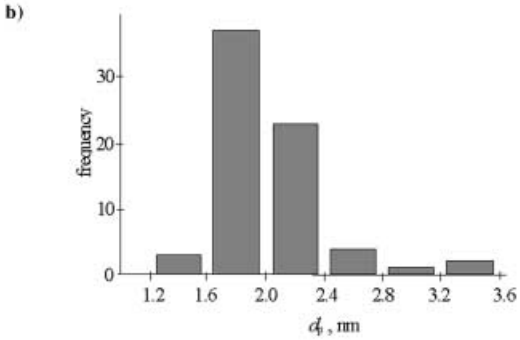

Figure 3. Low-resolution TEM picture of MPIF$^-$Na$^+$/Pd^0 (above) and size distribution of the metal nanoclusters determined by computer image analysis (below).

Table 2. Nanomorphology of the investigated materials in water expressed in terms of cylindrical pores model.

D_{pr} [nm][a]	V_{pr} [cm^{3}g^{-1}][b]			
	MPIF(H)	MPIF$^-$Na$^+$	MPIF$^-$Pd$^{2+}{}_{0.5}$	MPIF$^-$Na$^+$/Pd^0
13.2	0.04	0	0	0
8.1	0	0	0.23	0.09
4.3	0.42	0.84	0.17	0.17
3.2	1.54	1.54	1.28	1.76
2.7	0	0	0	0
1.6	0	0	0	0
1.1	0	0	0	0
0.6	0.71	0.47	1.22	1.12

[a] Pore diameter. [b] Volume of a resin domain with pores of given diameter.

diameter produced upon reducing MPIF$^-$Pd$^{2+}{}_{0.5}$ in methanol (ca. 2 nm) appears a convincing support of the conceptual model depicted in Figure 1.

Conclusion

In summary, previous preliminary observations on the possibility of controlling the size of Pd nanoclusters generated inside gel-type functional resins appear to be confirmed. Lightly cross-linked resins (2–6% mol) appear to be effective templates for generating metal nanoclusters with diameters of2–3 nm, that is, a size that is typical of industrially relevant supported metal catalysts.

Experimental Section

Apparatus: SEM and XRMA, Cambridge Stereoscan 250 EDX PW 9800; TEM, JEOL 2010 with GIF; ESR, X-band JEOL JES-RE1X apparatus at 9.2 GHz (modulation 100 KHz) equipped with a variable temperature unit Steler. ISEC measurements were carried out by using an established procedure and a standard chromatographic set-up described elsewhere.[12] Samples for TEM analysis were prepared by extensive grinding of the as-prepared material to be examined; this was subsequently ultrasonically dispersed in methanol and then transferred as a suspension to a copper grid covered with a lacey carbon film.

Solvents and chemicals: Solvents and chemicals, from various commercial sources, were of reagent grade and were used as received. Methacrylic acid (MA), *N,N′*-dimethylacrylamide (DMAA) and *N,N′*-methylene bisacrylamide (MBAA) were from Polysciences.

Synthesis of MPIF$^-$Na$^+$/Pd^0: In a typical experiment, DMAA (17.40 g, 87.90% mol), (1.37 g MA , 7.97% mol), and MBAA (1.27 g, 4.13% mol) were mixed in a cylindrical glass vessel to give a clear colorless solution, which, after oxygen removal by means of nitrogen bubbling, underwent γ-irradiation (^{60}Co) for 18 h, at a distance of 17.1 cm from the source (total dose was ca. 10 KGy), at room temperature. The solution was transformed into a transparent pale yellow cylindrical block, which was triturated in methanol, washed with methanol (3×50 mL), and dried at 70 °C under about 5 mbar pressure. The polymerization yield was 96%. The resin was fully ground with an IKA A 10 impact grinder, sieved to 180–400 μm, re-washed with methanol (3×50 mL), and re-dried as above. Volumetric acid–base titration gave approximately 0.72 meq H$^+$g^{-1}. Elemental analysis was consistent with the expected composition. Palladiation and reduction of Pd^{II} to Pd^0 were carried out as described in previous papers.[3, 7] Pd content was found to be 2.45%.

Acknowledgement

We are indebted to Dr. P. Guerriero, CNR Padova, for XRMA analysis, and to Dr. A. Venezia, CNR Palermo, for XPS analysis. This work was partially supported by P.R.I.N. funding, 2001–2003, Ministero dell'Università e della Ricerca Scientifica, Italy (project number 2001038991) and by funds of Slovak VEGA (project 1/9142/02).

[1] R. Wagner, P. M. Lange *Erdoel Erdgas Kohle* **1989**, *105*, 414–419.
[2] P. M. Lange, F. Martinola, S. Oeckel, *Hydrocarbon Process.* **1985**, *64*, 51–52.
[3] B. Corain, M. Králik, *J. Mol. Catal. A* **2000**, *159*, 153–162 (review paper).
[4] M. Králik, M. Hronec, S. Lora, G. Palma, M. Zecca, A. Biffis, B. Corain, *J. Mol. Catal.* **1995**, *97*, 145–155.
[5] A. Guyot in *Synthesis and Separations using Functional Polymers* (Eds.: D. C. Sherrington, P. Hodge), Wiley, New York, **1988**, pp. 1–42.
[6] B. Corain, M. Zecca, K. Jerabek, *J. Mol. Catal. A* **2001**, *177*, 3–20 (review paper).
[7] B. Corain, P. Centomo, S. Lora, M. Králik, *J. Mol. Catal. A*, in press (review paper).
[8] A. Biffis, R. Ricoveri, S. Campestrini, M. Králik, K. Jerabek, B. Corain, *Chem. Eur. J.* **2002**, *8*, 2962–2967.
[9] M. Králik, V. Kratky, M. De Rosso, M. Tonelli, S. Lora, B. Corain, *Chem. Eur. J.* **2003**, *9*, 209–214.
[10] M. Králik, M. Hronec, V. Jorik, S. Lora, G. Palma, A. Biffis, B. Corain, *J. Mol. Catal. A* **1995**, *101*, 143–152.

[11] A. Biffis, A. A. D'Archivio, K. Jeràbek, G. Schmid, B. Corain, *Adv. Mater.* **2000**, *12*, 1909 – 1912.
[12] K. Jerabek, *Anal. Chem*. **1985**, *57*, 1598.
[13] G. Ogston, *Trans. Faraday Soc.* **1958**, *54*, 1754 – 1757.
[14] "Cross Evaluation of Strategies in Size-Exclusion Chromatography": K. Jerabek, *ACS Symp. Ser.* **1996**, *635*, 211 – 220.
[15] Dr A. Venezia, CNR Palermo, Italy, personal communication.
[16] M. J. Yacaman, M. M. Almazo, J. A. Ascencio, *J. Mol. Catal. A* **2001**, *173*, 61 – 74.
[17] A. Biffis, B. Corain, M. Zecca, C. Corvaja, K. Jerabek *J. Am. Chem. Soc.* **1995**, *117*, 1603 – 1606.
[18] A. A. D'Archivio, L. Galantini, A. Panatta, E. Tettamanti, B. Corain, *J. Phys. Chem. B* **1998**, *102* , 6774 – 6779, and references therein.

Received: March 19, 2003 [F4965]